Modulation of Photochemical Activity of Titania Nanosheets via Heteroassembly with Reduced Graphene Oxide. Enhancement of Photoinduced Hydrophilic Conversion Properties.

Nobuyuki Sakai,[†] Kei Kamanaka,[†,‡] and Takayoshi Sasaki[†,‡,*]

[†] International Center for Materials Nanoarchitectonics, National Institute for Materials Science, 1-1 Namiki, Tsukuba, Ibaraki 305-0044, Japan.

[‡] Graduate School of Pure and Applied Sciences, University of Tsukuba, 1-1-1 Tennodai, Tsukuba, Ibaraki 305-8571, Japan.

[*] Corresponding author

E-mail: sasaki.takayoshi@nims.go.jp

Abstract

The heteroassembly of two-dimensional (2D) nanosheets has attracted rapidly increasing attention for designing new materials and nanodevices, in which the properties of the individual components can be modulated through the concerted interaction between the different 2D nanosheets. Here, we report on the layer-by-layer integration of photofunctional titania nanosheets and conductive reduced graphene oxide (rGO) to enhance the photochemical activity of the titania nanosheets. Heteroassembled films were fabricated by sequentially assembling graphene oxide (GO) and titania nanosheets with a cationic polymer and subsequently exposing to UV light to reduce the GO. The films showed an accelerated photoinduced hydrophilic conversion, the rate of which was 2.8 times higher than that of a film solely of the titania nanosheets. This behavior indicates that the rGO worked as an electron transfer mediator and improved the photoinduced charge separation efficiency. The intimate contact between two different 2D nanosheets promotes the efficient utilization of photogenerated carriers.

Introduction

The integration of graphene, two-dimensional (2D) carbon material, with semiconducting materials has been extensively investigated in the field of photocatalysis during the last decade.[1-10] Because the graphene has lower Fermi level compared to the lower edge of the conduction band for various semiconductor photocatalysts such as TiO_2, ZnO, CdS, etc., the graphene works as an acceptor for electrons photogenerated in the semiconductor photocatalysts. In addition, the good electrical conductivity of graphene accelerates the migration of the electrons to suppress the recombination of electron-hole pairs. As a result, the semiconductor-graphene composite photocatalysts show improved charge separation efficiency, which promotes various photocatalytic reactions efficiently, including photocatalytic air/water purification,[11] water splitting,[12] CO_2 reduction,[13] antibacterial activity,[14] and photoinduced superhydrophilicity.[15] The reduced graphene oxide (rGO) is often used instead of graphene because of its easiness of handling. In these systems, however, there are difficulties in making uniform and large area contact between semiconducting materials and graphene in the composites, which are obtained by mixing the two components. To improve the photocatalytic activity of the semiconductor-graphene composite photocatalysts, it is necessary to make good contact with large interface area between semiconducting materials and graphene uniformly at the molecular scale.

Another 2D materials, metal oxide nanosheets, have also attracted significant attention because of their unique structural, electronic, and morphological features.[16-20] The oxide nanosheets, which are derived from their parent layered crystals via exfoliation, possess an ultrathin thickness of a few nanometers, and their lateral size ranges from submicrometers to several tens of micrometers. Because of such a molecularly thin 2D structure, the oxide nanosheets show unique properties that differ from those of the bulk and nanoparticles. In recent decades, it has been reported that various types of oxide nanosheets exhibit a range of functionalities, such as robust high-*k* dielectric properties,[21-23] magneto-optical effects,[24] energy storage abilities,[25,26] and electrochromism.[27] Among these nanosheets,

titania nanosheets are particularly attractive because of various useful properties, including photofunctionality.[19,28-31] We have reported that titania nanosheets work as photoelectrodes,[32] which generate an anodic photocurrent by a bandgap excitation. Titania nanosheets and some other oxide nanosheets yielded photoinduced superhydrophilicity[33-36] and photocatalytic abilities[30,31,37-40] under ultraviolet (UV) irradiation.

The heteroassembly of two different types of 2D nanosheets has emerged as a fascinating route to novel artificial materials and systems, which evolve new or enhanced functionalities through the cooperative action of the components' different properties.[41-45] In our previous study, we demonstrated that an alternate assembly of Co-substituted titania nanosheets and Fe-substituted titania nanosheets has resulted in a significantly enhanced magneto-optical response in comparison with that from either individual film.[24] Heteroassembly of oxide nanosheets with graphene is of significant interest,[46-48] but such studies are still limited and, in particular, demonstration on molecular-level integration has been rare. Recently we have reported the layer-by-layer assembly of graphene oxide (GO) and its reduced form with titania nanosheets and found that the fabricated films show efficient photoinduced charge accumulation.[49,50] On the basis of these results, control of photochemical activity of oxide nanosheets via integration with GO (rGO) would be very attractive research target, although there have been no reports up to now, to the best of our knowledge.

In the present study, we constructed a heteroassembled film composed of titania nanosheets and rGO, expecting an improvement of the photoinduced hydrophilic conversion activity of the titania nanosheets. The photoinduced superhydrophilicity is one of the most important properties of semiconductor photocatalysts for practical applications.[51-56] This property yields anti-fogging effects and self-cleaning effects, which can be used for environmental mediation, indoor furnishing, and building materials. In a previous study,[33] we reported that the photoinduced superhydrophilicity was attained on a monolayer film of titania nanosheets, while lower activity was observed in 5- and

10-layer films of titania nanosheets in comparison to a monolayer film. This behavior can be understood by the fact that photogenerated electrons and holes predominantly undergo recombination while migrating to the topmost surface through the multilayer films. To improve the properties of the system, the photogenerated holes, which are responsible for inducing the hydrophilic conversion,[53-56] should be preferentially concentrated in the topmost titania layer of the films. Therefore, we employed rGO in this study, which may work as an acceptor of electrons generated in the titania nanosheets under UV irradiation.[50] It is anticipated that the electron transfer is facilitated by the large interface area between the two types of nanosheets to improve the charge separation efficiency, ultimately enhancing the hydrophilic conversion rate of the titania nanosheets.

Experimental

Synthesis of nanosheet suspensions. A colloidal suspension of $Ti_{0.87}O_2^{0.52-}$ nanosheets was prepared according to previously reported procedures.[57,58] Briefly, a mixture of TiO_2, K_2CO_3, and Li_2CO_3 powders (TiO_2:K_2CO_3:Li_2CO_3 = 1:0.23:0.078 in mole) was heated at 1173 K in air for 1 h. After cooling, the powder was ground and annealed at 1273 K for 20 h to obtain a pure phase of $K_{0.8}Ti_{1.73}Li_{0.27}O_4$. The obtained $K_{0.8}Ti_{1.73}Li_{0.27}O_4$ was dispersed and stirred in a 1 M HCl solution at ambient temperature for 3 days to yield a protonated phase, $H_{1.07}Ti_{1.73}O_4{\cdot}H_2O$. The obtained $H_{1.07}Ti_{1.73}O_4{\cdot}H_2O$ was exfoliated by agitating for one week in a tetrabutylammonium (TBA) hydroxide solution with a concentration adjusted to a molar ratio of TBA^+/H^+ = 1. The resulting suspension contained negatively charged unilamellar nanosheets of $Ti_{0.87}O_2^{0.52-}$ having an average lateral size of ~400 nm.

Graphene oxide (GO) nanosheet suspensions were prepared from natural graphite flake (Wako, >98.0% purity, and 15 μm in diameter) using a modified Hummers' method.[59,60] Briefly, 1 g of graphite, 1.2 g of KNO_3 (Wako, 99.0%), and 50 cm^3 of H_2SO_4 (Wako, 95%) were mixed in a 1000 cm^3 beaker.

Then, 6 g of $KMnO_4$ (Wako, 99.3%) was slowly added. The solution was stirred for 6 h at room temperature. Subsequently, after the temperature of the solution was increased to 80 °C, 20 cm^3 of water was added dropwise to avoid further rise in temperature. Then, 100 cm^3 of water was added to further dilute the suspension, followed by the slow addition of 6 cm^3 of H_2O_2 (Wako, 30 wt%). After the solution was cooled to room temperature, the resulting precipitate was diluted to 1000 cm^3 with water and stood still for several hours to allow for sedimentation. Then, the supernatant was decanted. The decantation and the dilution were repeated several times until the pH of the solution was ~4. The resulting solution was ultrasonicated for 1 h to yield the suspension containing negatively charged GO nanosheets.

Film Fabrication. Quartz glass and Si wafer substrates were cleaned by immersing in a bath of methanol/HCl (1:1 in volume) and then in concentrated H_2SO_4, for 30 min each. Multilayer films were fabricated via the sequential adsorption procedure.[61] First, the substrate was immersed in an aqueous solution of polydiallyldimethylammonium chloride (PDDA, 20 g dm^{-3}, and pH = 9) to turn the surface positively charged. Then, the PDDA-coated substrate was immersed in a colloidal suspension of nanosheets (0.06 g dm^{-3} and 0.10 g dm^{-3} for the $Ti_{0.87}O_2^{0.52-}$ and GO nanosheet suspensions, respectively, pH = 9). The substrate was immersed in each solution for 20 min and then rinsed thoroughly with ultrapure water.

Characterization. Atomic force microscopy (AFM) images were collected in tapping-mode using a SII NanoNavi II Station and a cantilever (SI-DF20, SII) to examine the topography of the nanosheets deposited onto a Si wafer substrate. A spectrophotometer (U-4100, Hitachi) was employed to record the UV-vis absorption spectra. A contact angle meter (CA-XP, Kyowa Interface Science) was employed to evaluate the wettability of the sample surfaces. A 500 W Xe lamp (XEF-501S, Sanei-Electric) equipped with cold mirrors that do not reflect light with a wavelength of >500 nm was employed as a UV light source. The light intensity was calibrated with a spectroradiometer (USR-45, Ushio).

Results and Discussion

$Ti_{0.87}O_2^{0.52-}$ and graphene oxide (GO) nanosheet suspensions were prepared according to previously reported procedures.[57-60] The obtained nanosheets were assembled into a monolayer film using the layer-by-layer assembly method.[61] We observed the films fabricated on a Si wafer by atomic force microscopy (AFM) as shown in **Figure 1**. The thickness of the $Ti_{0.87}O_2^{0.52-}$ nanosheets was estimated as ~1.2 nm, and the lateral size ranged from 100 nm to 800 nm. The surface coverage was 85%, and the overlapped area was 41% in the monolayer film of the $Ti_{0.87}O_2^{0.52-}$ nanosheets. In contrast, the thickness of the graphene oxide (GO) nanosheets was estimated as ~0.98 nm, and the lateral size ranged from 300 nm to 1700 nm. The surface coverage and overlapped area were 97% and 70%, respectively, in the monolayer film of GO nanosheets. Although there were uncoated or overlapped areas, a substantial monolayer film was formed in each case.

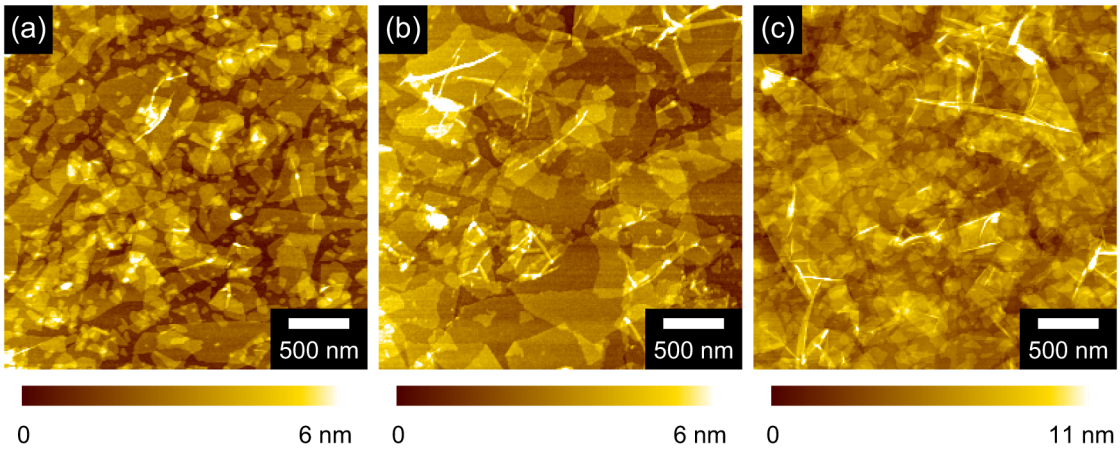

Figure 1. AFM images of films of (a) substrate/PDDA/$Ti_{0.87}O_2^{0.52-}$, (b) substrate/PDDA/GO, and (c) substrate/PDDA/GO/PDDA/$Ti_{0.87}O_2^{0.52-}$. Si wafers were used as substrates.

To fabricate a heteroassembled film, a monolayer film of GO nanosheets was covered with PDDA

and then with the $Ti_{0.87}O_2^{0.52-}$ nanosheets. The AFM image suggests the presence of two types of nanosheets (**Figure 1c**). In addition, UV-vis absorption spectra clearly supported the successful formation of the heteroassembled film on a quartz substrate. Monolayer films of $Ti_{0.87}O_2^{0.52-}$ (**Figure 2**, blue line) and GO (**Figure 2**, green line) nanosheets yielded absorption peaks at 265 nm and 230 nm, respectively. The absorbance at the peak wavelengths was 0.19 and 0.03, which is consistent with that reported in a previous paper.[49] The absorbance of the heteroassembled film (**Figure 2**, red line) was nearly equal to the sum of the absorbance of the monolayer films of the $Ti_{0.87}O_2^{0.52-}$ nanosheets and GO nanosheets. On the basis of the above results, it is confirmed that the heteroassembled film of substrate/PDDA/GO/PDDA/$Ti_{0.87}O_2^{0.52-}$ is composed of the monolayer film of the $Ti_{0.87}O_2^{0.52-}$ nanosheets assembled on top of the monolayer film of the GO nanosheets with an intervening layer of PDDA at the molecular level.

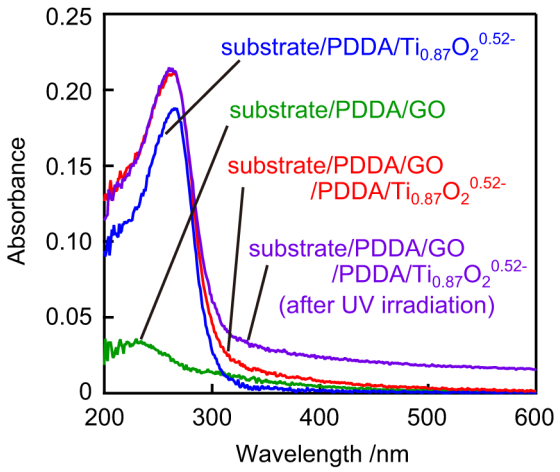

Figure 2. UV-vis absorption spectra of monolayer films of substrate/PDDA/$Ti_{0.87}O_2^{0.52-}$ (blue line) and substrate/PDDA/GO (green line), a heteroassembled film of substrate/PDDA/GO/PDDA/$Ti_{0.87}O_2^{0.52-}$ (red line), and the heteroassembled film after UV irradiation (1 mW/cm^2) for 48 h (purple line).

The obtained heteroassembled film of substrate/PDDA/GO/PDDA/$Ti_{0.87}O_2^{0.52-}$ was exposed to UV

light (<300 nm, 1 mW/cm^2, and 48 h) for the reduction of the GO nanosheets as well as the removal of the PDDA layers. Upon UV irradiation, we observed a broad enhancement of the absorbance in the visible range (**Figure 2**, purple line), which is characteristic of rGO,[63,64] whereas the spectral profile at 300 nm and below did not change. This enhancement indicates that the GO layer was photocatalytically reduced to rGO by the injection of excited electrons generated in the $Ti_{0.87}O_2^{0.52-}$ layer under UV irradiation.[49,65] The reduction of GO is also confirmed by the change of carbon (1s) X-ray photoelectron spectroscopy (XPS) data (Supporting Information, **Figure S1**). The relative intensity of oxygen-containing carbon groups compared to the total intensity of carbon became small after the UV irradiation. The UV irradiation also causes decomposition of PDDA into NH_4^+ or H^+ by the photocatalytic action of the $Ti_{0.87}O_2^{0.52-}$ nanosheets according to our previous reports.[49,62] The removal of the PDDA layers has been confirmed by the decrease of the *d*-spacing of 002 peak associated with the separation between GO and $Ti_{0.87}O_2^{0.52-}$ nanosheets.[49] As a result, we obtained polymer-free bilayer films composed of monolayers of $Ti_{0.87}O_2^{0.52-}$ and rGO, or substrate/rGO/$Ti_{0.87}O_2^{0.52-}$.

The fabricated films showed superhydrophilicity because of the pre-irradiation. Prior to the wettability conversion measurements, the films were heated (100 °C, 48 h, and in air) to turn their surface hydrophobic,[66] yielding a water contact angle greater than 40°. Then, we performed photoinduced wettability conversion tests. For both the heteroassembled film and the monolayer film of the $Ti_{0.87}O_2^{0.52-}$ nanosheets, the water contact angle gradually decreased to ~5° under UV irradiation (10 mW/cm^2, in air); however, the former attained the superhydrophilic state in a shorter period of time (**Figure 3a**). The empirically defined rate[54] for the hydrophilic conversion, as estimated by taking the slope of the plots for the reciprocal of the contact angle[67] and the irradiation time, was 1.2×10^{-2} and 4.3×10^{-3} degree^{-1} min^{-1} for the heteroassembled film and the monolayer film, respectively (**Figure 3b**).

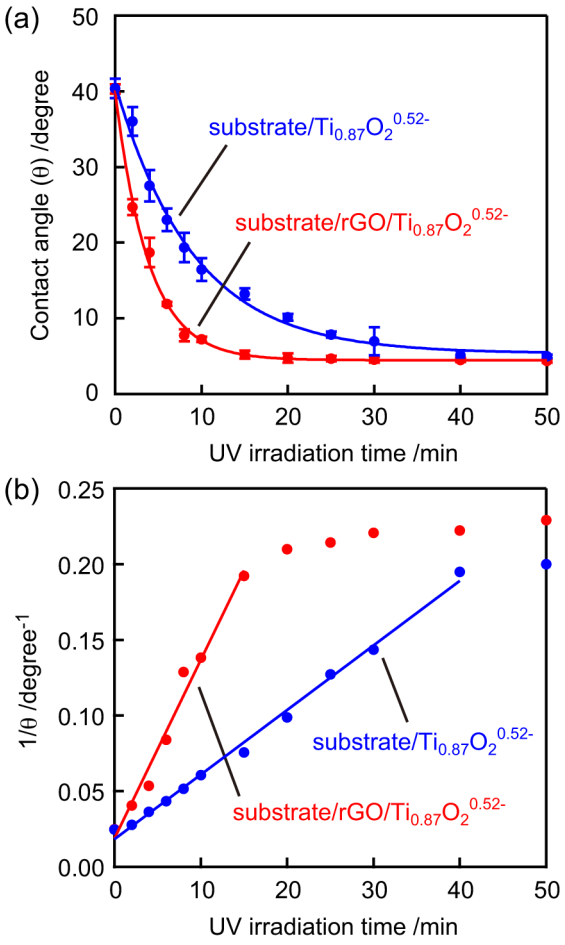

Figure 3. Changes in (a) contact angle and (b) its reciprocal for the monolayer film of substrate/$Ti_{0.87}O_2^{0.52-}$ (blue circles) and the heteroassembled film of substrate/rGO/$Ti_{0.87}O_2^{0.52-}$ (red circles) under UV light irradiation (10 mW/cm^2, in air).

We also examined the hydrophilic conversion of the films under various intensities of UV light, and the hydrophilic conversion rate is plotted against the UV light intensity (**Figure 4**, filled circles). Similar to our previous observations for the monolayer film of $Ti_{0.91}O_2^{0.36-}$ nanosheets,[33] the heteroassembled film yielded a linear relationship with a slope of ~1 between the logarithms of the hydrophilic conversion rate and the light intensity. This result suggests that the wettability conversion proceeded under light-limiting conditions, even when the intensity was as high as 30 mW/cm^2, where

the recombination of photogenerated carriers usually prevails, as was actually observed for 5- and 10-layer films of the $Ti_{0.91}O_2^{0.36-}$ nanosheets.[33] More importantly, the rate for the heteroassembled film was 2.8 times larger than that for the monolayer film of the $Ti_{0.87}O_2^{0.52-}$ nanosheets. The heterojunction of rGO and $Ti_{0.87}O_2^{0.52-}$ nanosheets accelerates the hydrophilic conversion of the film surfaces.

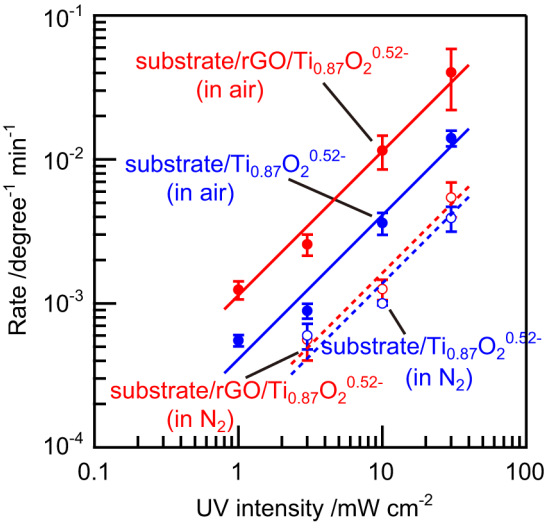

Figure 4. Dependence of photoinduced hydrophilic conversion rate on the UV light intensity: a monolayer film of substrate/$Ti_{0.87}O_2^{0.52-}$ (blue circles) and a heteroassembled film of substrate/rGO/$Ti_{0.87}O_2^{0.52-}$ (red circles). The UV irradiation was performed in ambient air (filled circles) or a humid N_2 atmosphere (open circles).

The enhancement of the hydrophilic conversion rate is ascribable to the improvement in charge separation efficiency because the rGO layer may work as an electron acceptor. To investigate the role of the rGO layer in more detail, we examined the hydrophilic conversion of the heteroassembled film and the monolayer film of $Ti_{0.87}O_2^{0.52-}$ nanosheets under a humid N_2 atmosphere. Both of the films showed fairly slow wettability change in a humid N_2 atmosphere compared with in air (Supporting Information, **Figure S2**). The extent of the suppression in activity was much higher for the

heteroassembled film, and the rates in N_2 were similar to each other (**Figure 4**, open circles). These results suggest that the rGO layer does not accumulate electrons transferred from the $Ti_{0.87}O_2^{0.52-}$ nanosheets, which is different from the case of the photoinduced enhancement in conductivity of $(rGO/Ti_{0.87}O_2^{0.52-})_n$-based field-effect transistor in our previous report,[50] and that the O_2 molecules in the air are indispensable for the hydrophilic conversion. Without O_2 molecules, the electrons that are injected into the rGO layer in the heteroassembled film might transfer back to the $Ti_{0.87}O_2^{0.52-}$ nanosheets and recombine with the remaining holes. Hence, we conclude that the rGO layer works as an electron transfer mediator and enhances the charge separation efficiency, which results in the efficient utilization of holes for hydrophilic conversion.

The fact that the rGO layer works as an electron transfer mediator can be supported by the difference of energy levels for each component as shown in **Figure 5**. Since the work function of rGO has been determined by ultraviolet photoemission spectroscopy as ~4.36 eV vs. vacuum[68] (-0.08 V vs. SHE), excited electrons in the conduction band of anatase TiO_2 (-0.16 V vs. SHE[69,70]) can be injected into rGO in the TiO_2-rGO composites.[68,71] The conduction band edge for the $Ti_{0.91}O_2^{0.36-}$ nanosheets is more negative by 0.12 V than that for anatase TiO_2,[32] and thus excited electrons in the $Ti_{0.87}O_2^{0.52-}$ nanosheets are also possible to transfer to the rGO layer. On the other hand, O_2 molecules can be reduced to HO_2 at the potential of -0.046 V vs. SHE,[72] which is more positive than the Fermi level of rGO. Hence, excited electrons in the $Ti_{0.87}O_2^{0.52-}$ nanosheets under UV light can be transferred to O_2 molecules through the rGO layer in the present system.

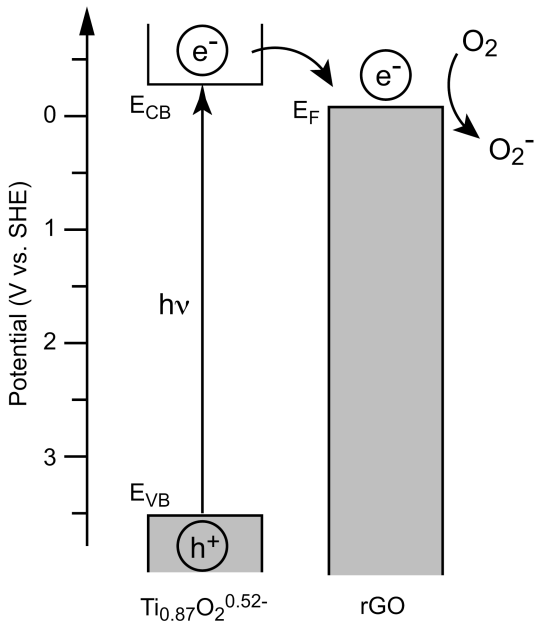

Figure 5. Schematic energy level diagram of rGO/$Ti_{0.87}O_2^{0.52-}$. E_{CB} and E_{VB} denote the conduction band edge and the valence band edge of $Ti_{0.87}O_2^{0.52-}$ nanosheets, respectively, and E_F denotes the Fermi level of rGO.

When considered from a different point of view regarding the results shown in **Figure S2**, the presence of O_2 in air accelerates the hydrophilic conversion for both the heteroassembled film and the monolayer film. It is noteworthy that the increase in the rate for the monolayer film (3 times) was not significant compared with that observed for the heteroassembled film (7 times). This suggests that the electron transfer from the $Ti_{0.87}O_2^{0.52-}$ nanosheets to the O_2 molecules in air occurs more easily when the rGO layer is present beneath the layer of $Ti_{0.87}O_2^{0.52-}$ nanosheets. This is probably due to the intimate contact between the $Ti_{0.87}O_2^{0.52-}$ nanosheets and the rGO nanosheets because of their two-dimensional nature.

We also examined the effect of the rGO layer on the hydrophilic conversion of multilayer films of $Ti_{0.87}O_2^{0.52-}$ nanosheets. We fabricated heteroassembled films composed of multilayer films of the $Ti_{0.87}O_2^{0.52-}$ nanosheets on top of the monolayer film of rGO, substrate/rGO/$(Ti_{0.87}O_2^{0.52-})_n$ (n = 2 and 5),

as well as multilayer films of the $Ti_{0.87}O_2^{0.52-}$ nanosheets (substrate/$(Ti_{0.87}O_2^{0.52-})_n$, n = 2 and 5) by similar procedures involving layer-by-layer assembly and subsequent UV irradiation. The 2-layer film of the $Ti_{0.87}O_2^{0.52-}$ nanosheets showed a small increase in the rate (~1.1 times) by integrating with the rGO layer, whereas the 5-layer film did not. These results may indicate that the excited electrons generated in the $Ti_{0.87}O_2^{0.52-}$ nanosheets can effectively transfer to the rGO layer only when the $Ti_{0.87}O_2^{0.52-}$ nanosheets are in direct contact with the rGO layer.

We also fabricated heteroassembled films composed of two layers of rGO nanosheets underneath a monolayer of $Ti_{0.87}O_2^{0.52-}$ nanosheets, substrate/$(rGO)_2$/$Ti_{0.87}O_2^{0.52-}$. The hydrophilic conversion rate for substrate/$(rGO)_2$/$Ti_{0.87}O_2^{0.52-}$ was 1.0×10^{-2} degree^{-1} min^{-1} at the intensity of 10 mW/cm^2, which is similar to that for substrate/rGO/$Ti_{0.87}O_2^{0.52-}$. Hence, no more enhancement in photochemical activity of rGO/$Ti_{0.87}O_2^{0.52-}$ composites was obtained by integrating with another layer of rGO, suggesting that one layer of rGO nanosheets is enough to enhance the charge separation efficiency.

Several groups have reported on the photocatalytic decomposition of rGO by TiO_2 such as anatase.[73-75] Thus, we also examined the stability of GO as well as rGO in the heteroassembled film of substrate/PDDA/GO/PDDA/$Ti_{0.87}O_2^{0.52-}$ in comparison with that in a reversely stacked film, substrate/PDDA/$Ti_{0.87}O_2^{0.52-}$/PDDA/GO, against UV irradiation. In the case of the latter film, the water contact angle (**Figure 6a**, blue circles) and the absorbance in the visible range (**Figure 6b**, blue circles) increased during the initial several hours, and then both of the contact angle and the absorbance decreased. The initial increase in the contact angle was due to the removal of the oxygen-containing groups in GO, resulting in the appearance of the hydrophobic nature of rGO.[76] This is consistent with the enhancement of the absorbance throughout the visible-light range, which is characteristic of rGO. The prolonged UV irradiation may have eventually led to the photocatalytic decomposition of rGO and the gradual exposure of the $Ti_{0.87}O_2^{0.52-}$ surface to air, which promoted the superhydrophilicity of the film surface. The decomposition of rGO is also supported by a decrease in absorbance for the visible

range. In contrast, substrate/PDDA/GO/PDDA/$Ti_{0.87}O_2^{0.52-}$ showed a different behavior. The contact angle monotonically decreased to show the superhydrophilicity (**Figure 6a**, red circles). The absorbance in visible-light range was enhanced during the initial several hours of irradiation and then remained nearly constant, indicating the formation of rGO (**Figure 6b**, red circles). When the rGO layer is on top of the $Ti_{0.87}O_2^{0.52-}$ layer (substrate/$Ti_{0.87}O_2^{0.52-}$/rGO) and most of the rGO surface is exposed to air, the rGO layer is easily decomposed by the photocatalytic activity of $Ti_{0.87}O_2^{0.52-}$ because of the easy contact with O_2 and H_2O, which are sources of active oxygen species. In contrast, in substrate/rGO/$Ti_{0.87}O_2^{0.52-}$, the $Ti_{0.87}O_2^{0.52-}$ layer protected the rGO layer from the ambient atmosphere and photocatalytic decomposition. Reversible hydrophilic/hydrophobic conversion was observed at least up to 7 cycles without dramatic changes in the absorption spectra of the films.

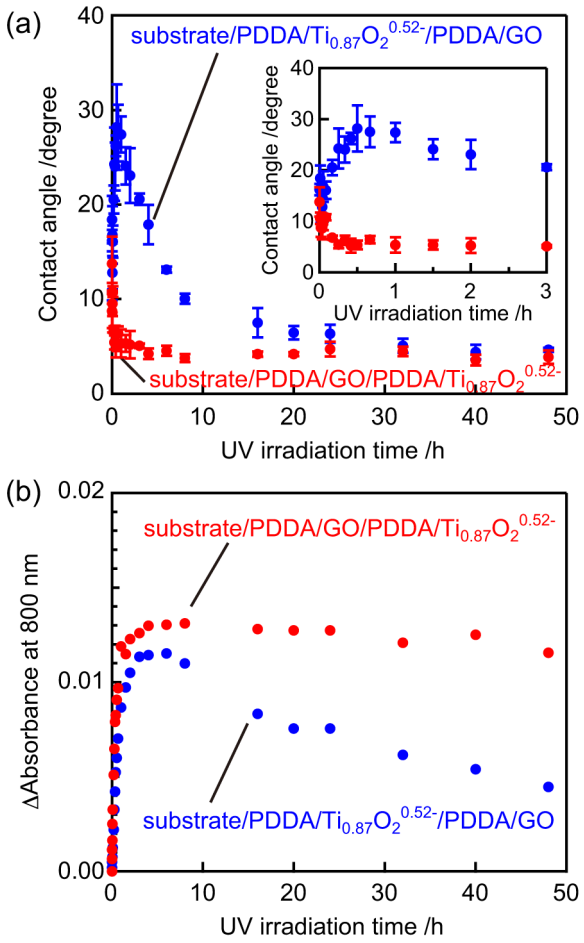

Figure 6. Changes in (a) contact angle and (b) absorbance for substrate/PDDA/$Ti_{0.87}O_2^{0.52-}$/PDDA/GO (blue circles) and substrate/PDDA/GO/PDDA/$Ti_{0.87}O_2^{0.52-}$ (red circles) under UV irradiation (<300 nm, 1 mW/cm^2). Inset in (a) shows an expanded figure in the initial stage of UV irradiation.

Conclusions

We achieved the modulation of photochemical activity of the titania nanosheets by introducing an underlying film of rGO; photoinduced hydrophilic conversion properties of the titania nanosheets were enhanced. The rGO layer served as an efficient mediator for the electron transfer from the titania nanosheets to the O_2 molecules in air because of the intimate 2D contact between the two layers. The stacked heteronanostructure is promising for designing various photofunctional materials, including

photocatalysts, because of the efficient charge separation at the interface between two types of 2D materials.

Acknowledgment. This work was partly supported by the World Premier International Research Center Initiative on Materials Nanoarchitectonics (WPI-MANA), MEXT, Japan. N.S. acknowledges support from JSPS KAKENHI Grant Number JP16K14428.

Supporting Information. X-ray photoelectron spectroscopy (XPS) data for heteroassembled films of $Ti_{0.87}O_2^{0.52-}$ and GO nanosheets and changes of contact angle in N_2 atmosphere.

References and notes

(1) Kamat, P. V. Graphene-Based Nanoassemblies for Energy Conversion. *J. Phys. Chem. Lett.* **2011**, *2*, 242-251.

(2) An, X.; Yu, J. C. Graphene-Based Photocatalytic Composites. *RSC Adv.* **2011**, *1*, 1426-1434.

(3) Xiang, Q.; Yu, J.; Jaroniec, M. Graphene-Based Semiconductor Photocatalysts. *Chem. Soc. Rev.* **2012**, *41*, 782-796.

(4) Han, L.; Wang, P.; Dong, S. Progress in Graphene-Based Photoactive Nanocomposites as a Promising Class of Photocatalyst. *Nanoscale* **2012**, *4*, 5814-5825.

(5) Lightcap, I. V.; Kamat, P. V. Graphitic Design: Prospects of Graphene-Based Nanocomposites for Solar Energy Conversion, Storage, and Sensing. *Acc. Chem. Res.* **2013**, *46*, 2235-2243.

(6) Tu, W.; Zhou, Y.; Zou, Z. Versatile Graphene-Promoting Photocatalytic Performance of Semiconductors: Basic Principles, Synthesis, Solar Energy Conversion, and Environmental Applications. *Adv. Funct. Mater.* **2013**, *23*, 4996-5008.

(7) Xiang, Q.; Yu, J. Graphene-Based Photocatalysts for Hydrogen Generation. *J. Phys. Chem. Lett.*

2013, *4*, 753-759.

(8) Xie, G.; Zhang, K.; Guo, B.; Liu, Q.; Fang, L.; Gong, J. R. Graphene-Based Materials for Hydrogen Generation from Light-Driven Water Splitting. *Adv. Mater.* **2013**, *25*, 3820-3839.

(9) Gao, N.; Fang, X. S. Synthesis and Development of Graphene-Inorganic Semiconductor Nanocomposites. *Chem. Rev.* **2015**, *115*, 8294-8343.

(10) Zhang, N.; Yang, M.-Q.; Liu, S.; Sun, Y.; Xu, Y.-J. Waltzing with the Versatile Platform of Graphene to Synthesize Composite Photocatalysts. *Chem. Rev.* **2015**, *115*, 10307-10377.

(11) Zhang, Y.; Tang, Z.-R.; Fu, X.; Xu, Y.-J. TiO_2-Graphene Nanocomposites for Gas-Phase Photocatalytic Degradation of Volatile Aromatic Pollutant: Is TiO_2-Graphene Truly Different from Other TiO_2-Carbon Composite Materials? *ACS Nano* **2010**, *4*, 7303-7314.

(12) Iwase, A.; Ng, Y. H.; Ishiguro, Y.; Kudo, A.; Amal, R. Reduced Graphene Oxide as a Solid-State Electron Mediator in Z-Scheme Photocatalytic Water Splitting under Visible Light. *J. Am. Chem. Soc.* **2011**, *133*, 11054-11057.

(13) Liang, Y. T.; Vijayan, B. K.; Gray, K. A.; Hersam, M. C. Minimizing Graphene Defects Enhances Titania Nanocomposite-Based Photocatalytic Reduction of CO_2 for Improved Solar Fuel Production. *Nano Lett.* **2011**, *11*, 2865-2870.

(14) Akhavan, O.; Ghaderi, E. Photocatalytic Reduction of Graphene Oxide Nanosheets on TiO_2 Thin Film for Photoinactivation of Bacteria in Solar Light Irradiation. *J. Phys. Chem. C* **2009**, *113*, 20214-20220.

(15) Anandan, S.; Rao, T. N.; Sathish, M.; Rangappa, D.; Honma, I.; Miyauchi, M. Superhydrophilic Graphene-Loaded TiO_2 Thin Film for Self-Cleaning Applications. *ACS Appl. Mater. Interfaces* **2013**, *5*, 207-212.

(16) Schaak, R. E.; Mallouk, T. E. Perovskites by Design: A Toolbox of Solid-State Reactions. *Chem. Mater.* **2002**, *14*, 1455-1471.

(17) Sasaki, T. Fabrication of Nanostructured Functional Materials Using Exfoliated Nanosheets as a Building Block. *J. Ceram. Soc. Jpn.* **2007**, *115*, 9-16.

(18) Osada, M.; Sasaki, T. Exfoliated Oxide Nanosheets: New Solution to Nanoelectronics. *J. Mater. Chem.* **2009**, *19*, 2503-2511.

(19) Ma, R.; Sasaki, T. Nanosheets of Oxides and Hydroxides: Ultimate 2D Charge-Bearing Functional Crystallites. *Adv. Mater.* **2010**, *22*, 5082-5104.

(20) Ma, R.; Sasaki, T. Two-Dimensional Oxide and Hydroxide Nanosheets: Controllable High-Quality Exfoliation, Molecular Assembly, and Exploration of Functionality. *Acc. Chem. Res.* **2015**, *48*, 136-143.

(21) Osada, M.; Ebina, Y.; Funakubo, H.; Yokoyama, S.; Kiguchi, T.; Takada, K.; Sasaki, T. High-*k* Dielectric Nanofilms Fabricated from Titania Nanosheets. *Adv. Mater.* **2006**, *18*, 1023-1027.

(22) Akatsuka, K.; Haga, M.; Ebina, Y.; Osada, M.; Fukuda, K.; Sasaki, T. Construction of Highly Ordered Lamellar Nanostructures through Langmuir-Blodgett Deposition of Molecularly Thin Titania Nanosheets Tens of Micrometers Wide and Their Excellent Dielectric Properties. *ACS Nano* **2009**, *3*, 1097-1106.

(23) Osada, M.; Akatsuka, K.; Ebina, Y.; Funakubo, H.; Ono, K.; Takada, K.; Sasaki, T. Robust High-*k* Response in Molecularly Thin Perovskite Nanosheets. *ACS Nano* **2010**, *4*, 5225-5232.

(24) Osada, M.; Ebina, Y.; Takada, K.; Sasaki, T. Gigantic Magneto-Optical Effects in Multilayer Assemblies of Two-Dimensional Titania Nanosheets. *Adv. Mater.* **2006**, *18*, 295-299.

(25) Sugimoto, W.; Iwata, H.; Yasunaga, Y.; Murakami, Y.; Takasu, Y. Preparation of Ruthenic Acid Nanosheets and Utilization of Its Interlayer Surface for Electrochemical Energy Storage. *Angew. Chem. Int. Ed.* **2003**, *42*, 4092-4096.

(26) Wang, C.; Osada, M.; Ebina, Y.; Li, B.-W.; Akatsuka, K.; Fukuda, K.; Sugimoto, W.; Ma, R.;

Sasaki, T. All-Nanosheet Ultrathin Capacitors Assembled Layer-by-Layer via Solution-Based Processes. *ACS Nano* **2014**, *8*, 2658-2666.

(27) Sakai, N.; Ebina, Y.; Takada, K.; Sasaki, T. Electrochromic Films Composed of MnO_2 Nanosheets with Controlled Optical Density and High Coloration Efficiency. *J. Electrochem. Soc.* **2005**, *152*, E384-E389.

(28) Gunjakar, J. L.; Kim, I. Y.; Lee, J. M.; Jo, Y. K.; Hwang, S.-J. Exploration of Nanostructured Functional Materials Based on Hybridization of Inorganic 2D Nanosheets. *J. Phys. Chem. C* **2014**, *118*, 3847-3863.

(29) Wang, L. Z.; Sasaki, T. Titanium Oxide Nanosheets: Graphene Analogues with Versatile Functionalities. *Chem. Rev.* **2014**, *114*, 9455-9486.

(30) Ida, S.; Ishihara, T. Recent Progress in Two-Dimensional Oxide Photocatalysts for Water Splitting. *J. Phys. Chem. Lett.* **2014**, *5*, 2533-2542.

(31) Luo, B.; Liu, G.; Wang, L. Z. Recent Advances in 2D Materials for Photocatalysis. *Nanoscale* **2016**, *8*, 6904-6920.

(32) Sakai, N.; Ebina, Y.; Takada, K.; Sasaki, T. Electronic Band Structure of Titania Semiconductor Nanosheets Revealed by Electrochemical and Photoelectrochemical Studies. *J. Am. Chem. Soc.* **2004**, *126*, 5851-5858.

(33) Sakai, N.; Fukuda, K.; Shibata, T.; Ebina, Y.; Takada, K.; Sasaki, T. Photoinduced Hydrophilic Conversion Properties of Titania Nanosheets. *J. Phys. Chem. B* **2006**, *110*, 6198-6203.

(34) Shibata, T.; Sakai, N.; Fukuda, K.; Ebina, Y.; Sasaki, T. Photocatalytic Properties of Titania Nanostructured Films Fabricated from Titania Nanosheets. *Phys. Chem. Chem. Phys.* **2007**, *9*, 2413-2420.

(35) Shibata, T.; Takanashi, G.; Nakamura, T.; Fukuda, K.; Ebina, Y.; Sasaki, T. Titanoniobate and

Niobate Nanosheet Photocatalysts: Superior Photoinduced Hydrophilicity and Enhanced Thermal Stability of Unilamellar Nb_3O_8 Nanosheet. *Energy Environ. Sci.* **2011**, *4*, 535-542.

(36) Katsumata, K.; Okazaki, S.; Cordonier, C. E. J.; Shichi, T.; Sasaki, T.; Fujishima, A. Preparation and Characterization of Self-Cleaning Glass for Vehicle with Niobia Nanosheets. *ACS Appl. Mater. Interfaces* **2010**, *2*, 1236-1241.

(37) Maeda, K.; Mallouk, T. E. Comparison of Two- and Three-Layer Restacked Dion-Jacobson Phase Niobate Nanosheets as Catalysts for Photochemical Hydrogen Evolution. *J. Mater. Chem.* **2009**, *19*, 4813-4818.

(38) Maeda, K.; Eguchi, M.; Oshima, T. Perovskite Oxide Nanosheets with Tunable Band-Edge Potentials and High Photocatalytic Hydrogen-Evolution Activity. *Angew. Chem. Int. Ed.* **2014**, *53*, 13164-13168.

(39) Compton, O. C.; Carroll, E. C.; Kim, J. Y.; Larsen, D. S.; Osterloh, F. E. Calcium Niobate Semiconductor Nanosheets as Catalysts for Photochemical Hydrogen Evolution from Water. *J. Phys. Chem. C* **2007**, *111*, 14589-14592.

(40) Osterloh, F. E. Inorganic Nanostructures for Photoelectrochemical and Photocatalytic Water Splitting. *Chem. Soc. Rev.* **2013**, *42*, 2294-2320.

(41) Osada, M.; Sasaki, T. Two-Dimensional Dielectric Nanosheets: Novel Nanoelectronics from Nanocrystal Building Blocks. *Adv. Mater.* **2012**, *24*, 210-228.

(42) Lotsch, B. V. Vertical 2D Heterostructures. *Annu. Rev. Mater. Res.* **2015**, *45*, 85-109.

(43) Ma, R.; Sasaki, T. Organization of Artificial Superlattices Utilizing Nanosheets as a Building Block and Exploration of Their Advanced Functions. *Annu. Rev. Mater. Res.* **2015**, *45*, 111-127.

(44) Kim, I. Y.; Jo, Y. K.; Lee, J. M.; Wang, L. Z.; Hwang, S.-J. Unique Advantages of Exfoliated 2D Nanosheets for Tailoring the Functionalities of Nanocomposites. *J. Phys. Chem. Lett.* **2014**, *5*, 4149-4161.

(45) Sakai, N.; Fukuda, K.; Omomo, Y.; Ebina, Y.; Takada, K.; Sasaki, T. Hetero-Nanostructured Films of Titanium and Manganese Oxide Nanosheets: Photoinduced Charge Transfer and Electrochemical Properties. *J. Phys. Chem. C* **2008**, *112*, 5197-5202.

(46) Manga, K. K.; Zhou, Y.; Yan, Y.; Loh, K. P. Multilayer Hybrid Films Consisting of Alternating Graphene and Titania Nanosheets with Ultrafast Electron Transfer and Photoconversion Properties. *Adv. Funct. Mater.* **2009**, *19*, 3638-3643.

(47) Tu, W.; Zhou, Y.; Liu, Q.; Tian, Z.; Gao, J.; Chen, X.; Zhang, H.; Liu, J.; Zou, Z. Robust Hollow Spheres Consisting of Alternating Titania Nanosheets and Graphene Nanosheets with High Photocatalytic Activity for CO_2 Conversion into Renewable Fuels. *Adv. Funct. Mater.* **2012**, *22*, 1215-1221.

(48) Yang, N.; Zhang, Y.; Halpert, J. E.; Zhai, J.; Wang, D.; Jiang, L. Granum-Like Stacking Structures with TiO_2-Graphene Nanosheets for Improving Photo-electric Conversion. *Small* **2012**, *8*, 1762-1770.

(49) Cai, X.; Ma, R.; Ozawa, T. C.; Sakai, N.; Funatsu, A.; Sasaki, T. Superlattice Assembly of Graphene oxide (GO) and Titania Nanosheets: Fabrication, In Situ Photocatalytic Reduction of GO and Highly Improved Carrier Transport. *Nanoscale* **2014**, *6*, 14419-14427.

(50) Cai, X.; Sakai, N.; Ozawa, T. C.; Funatsu, A.; Ma, R.; Ebina, Y.; Sasaki, T. Efficient Photoinduced Charge Accumulation in Reduced Graphene Oxide Coupled with Titania Nanosheets To Show Highly Enhanced and Persistent Conductance. *ACS Appl. Mater. Interfaces* **2015**, *7*, 11436-11443.

(51) Wang, R.; Hashimoto, K.; Fujishima, A.; Chikuni, M.; Kojima, E.; Kitamura, A.; Shimohigoshi, M.; Watanabe, T. Light-Induced Amphiphilic Surfaces. *Nature* **1997**, *388*, 431-432.

(52) Wang, R.; Hashimoto, K.; Fujishima, A.; Chikuni, M.; Kojima, E.; Kitamura, A.;

Shimohigoshi, M.; Watanabe, T. Photogeneration of Highly Amphiphilic TiO_2 Surfaces. *Adv. Mater.* **1998**, *10*, 135-138.

(53) Sakai, N.; Fujishima, A.; Watanabe, T.; Hashimoto, K. Enhancement of the Photoinduced Hydrophilic Conversion Rate of TiO_2 Film Electrode Surfaces by Anodic Polarization. *J. Phys. Chem. B* **2001**, *105*, 3023-3026.

(54) Sakai, N.; Fujishima, A.; Watanabe, T.; Hashimoto, K. Quantitative Evaluation of the Photoinduced Hydrophilic Conversion Properties of TiO_2 Thin Film Surfaces by the Reciprocal of Contact Angle. *J. Phys. Chem. B* **2003**, *107*, 1028-1035.

(55) Nakata, K.; Fujishima, A. TiO_2 Photocatalysis: Design and Applications. *J. Photochem. Photobiol. C* **2012**, *13*, 169-189.

(56) Liu, K.; Cao, M.; Fujishima, A.; Jiang, L. Bio-Inspired Titanium Dioxide Materials with Special Wettability and Their Applications. *Chem. Rev.* **2014**, *114*, 10044-10094.

(57) Sasaki, T.; Kooli, F.; Iida, M.; Michiue, Y.; Takenouchi, S.; Yajima, Y.; Izumi, F.; Chakoumakos, B. C.; Watanabe, M. A Mixed Alkali Metal Titanate with the Lepidocrocite-Like Layered Structure. Preparation, Crystal Structure, Protonic Form, and Acid-Base Intercalation Properties. *Chem. Mater.* **1998**, *10*, 4123-4128.

(58) Sasaki, T.; Watanabe, M. Osmotic Swelling to Exfoliation. Exceptionally High Degrees of Hydration of a Layered Titanate. *J. Am. Chem. Soc.* **1998**, *120*, 4682-4689.

(59) Hummers, W. S., Jr.; Offeman, R. E. Preparation of Graphitic Oxide. *J. Am. Chem. Soc.* **1958**, *80*, 1339-1339.

(60) Eda, G.; Fanchini, G.; Chhowalla, M. Large-Area Ultrathin Films of Reduced Graphene Oxide as a Transparent and Flexible Electronic Material. *Nat. Nanotechnol.* **2008**, *3*, 270-274.

(61) Sasaki, T.; Ebina, Y.; Tanaka, T.; Harada, M.; Watanabe, M.; Decher, G. Layer-by-Layer Assembly of Titania Nanosheet/Polycation Composite Films. *Chem. Mater.* **2001**, *13*,

4661-4667.

(62) Sasaki, T.; Ebina, Y.; Fukuda, K.; Tanaka, T.; Harada, M.; Watanabe, M. Titania Nanostructured Films Derived from a Titania Nanosheet/Polycation Multilayer Assembly via Heat Treatment and UV Irradiation. *Chem. Mater.* **2002**, *14*, 3524-3530.

(63) Shin, H.-J.; Kim, K. K.; Benayad, A.; Yoon, S.-M.; Park, H. K.; Jung, I.-S.; Jin, M. H.; Jeong, H.-K.; Kim, J. M.; Choi, J.-Y.; et al. Efficient Reduction of Graphite Oxide by Sodium Borohydride and Its Effect on Electrical Conductance. *Adv. Funct. Mater.* **2009**, *19*, 1987-1992.

(64) Zhang, Y.-L.; Guo, L.; Xia, H.; Chen, Q.-D.; Feng, J.; Sun, H.-B. Photoreduction of Graphene Oxides: Methods, Properties, and Applications. *Adv. Opt. Mater.* **2014**, *2*, 10-28.

(65) Williams, G.; Seger, B.; Kamat, P. V. TiO_2-Graphene Nanocomposites. UV-Assisted Photocatalytic Reduction of Graphene Oxide. *ACS Nano* **2008**, *2*, 1487-1491.

(66) Shibata, T.; Sakai, N.; Fukuda, K.; Ebina, Y.; Sasaki, T. Structural Study of Photoinduced Hydrophilicity of Titania Nanosheet Film. *Mater. Sci. Eng. B* **2009**, *161*, 12-15.

(67) It has been revealed that the reciprocal of contact angle is strongly correlated with the change of hydroxyl groups of TiO_2 surfaces (*J. Phys. Chem. B* **2003**, *107*, 1028). Hence, the empirically defined rate for the hydrophilic conversion stands for the rate of the change of hydroxyl groups.

(68) Tang, Y.-B.; Lee, C.-S.; Xu, J.; Liu, Z.-T.; Chen, Z.-H.; He, Z.; Cao, Y.-L.; Yuan, G.; Song, H.; Chen, L.; et al. Incorporation of Graphenes in Nanostructured TiO_2 Films via Molecular Grafting for Dye-Sensitized Solar Cell Application. *ACS Nano* **2010**, *4*, 3482-3488.

(69) Kavan, L.; Grätzel, M.; Gilbert, S. E.; Klemenz, C.; Scheel, H. J. Electrochemical and Photoelectrochemical Investigation of Single-Crystal Anatase. *J. Am. Chem. Soc.* **1996**, *118*, 6716-6723.

(70) Rothenberger, G.; Fitzmaurice, D.; Grätzel, M. Spectroscopy of Conduction Band Electrons in Transparent Metal Oxide Semiconductor Films: Optical Determination of the Flatband

Potential of Colloidal Titanium Dioxide Films. *J. Phys. Chem.* **1992**, *96*, 5983-5986.

(71) Wang, X.; Zhi, L.; Müllen, K. Transparent, Conductive Graphene Electrodes for Dye-Sensitized Solar Cells. *Nano Lett.* **2008**, *8*, 323-327.

(72) *Standard Potentials in Aqueous Solution*; Bard, A. J., Parsons, R., Jordan, J., Eds.; Marcel Dekker: New York, 1985.

(73) Akhavan, O.; Abdolahad, M.; Esfandiar, A.; Mohatashamifar, M. Photodegradation of Graphene Oxide Sheets by TiO_2 Nanoparticles after a Photocatalytic Reduction. *J. Phys. Chem. C* **2010**, *114*, 12955-12959.

(74) Zhang, L.; Diao, S.; Nie, Y.; Yan, K.; Liu, N.; Dai, B.; Xie, Q.; Reina, A.; Kong, J.; Liu, Z. Photocatalytic Patterning and Modification of Graphene. *J. Am. Chem. Soc.* **2011**, *133*, 2706-2713.

(75) Radich, J. G.; Krenselewski, A. L.; Zhu, J.; Kamat, P. V. Is Graphene a Stable Platform for Photocatalysis? Mineralization of Reduced Graphene Oxide With UV-Irradiated TiO_2 Nanoparticles. *Chem. Mater.* **2014**, *26*, 4662-4668.

(76) Sun, P.; Zhu, M.; Ma, R.; Wang, K.; Wei, J.; Wu, D.; Sasaki, T.; Zhu, H. Graphene Oxide/Titania Hybrid Films with Dual-UV-Responsive Surfaces of Tunable Wettability. *RSC Adv.* **2012**, *2*, 10829-10835.

TOC graphic

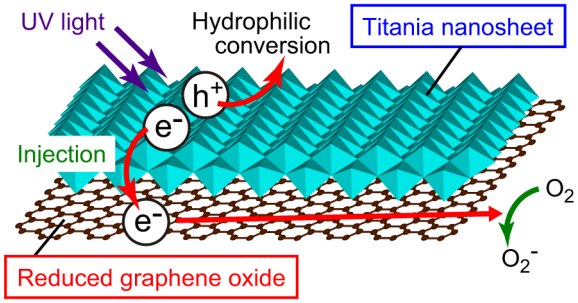
UV light
Hydrophilic conversion
Titania nanosheet
h+
e-
Injection
e-
O2
O2-
Reduced graphene oxide